Nanoscale patterning in application to materials and device structures

A. Erbe[a)]
Universität Konstanz, Fach M 676, Konstanz, D-78457, Germany

W. Jiang
Rutgers University, The State University of New Jersey, Piscataway, New Jersey 08855

Z. Bao
Stanford University, Stanford, California 94305

D. Abusch-Magder and D. M. Tennant
Bell Laboratories, Lucent Technologies, Murray Hill, New Jersey 07974

E. Garfunkel
Rutgers University, The State University of New Jersey, Piscataway, New Jersey 08855

N. Zhitenev
Bell Laboratories, Lucent Technologies, Murray Hill, New Jersey 07974

(Received 1 June 2005; accepted 3 October 2005; published 7 December 2005)

We present fabrication schemes for nanoscale molecular junctions, which allow the deposition of molecules after the fabrication steps that can uncontrollably affect the electrical properties of the molecular layers. The two techniques described here use shadow mask evaporation and nanotransfer printing. In order to make reliable contacts with the molecules (or molecular monolayers) the morphology of the contacting metals has to be optimized and controlled. We therefore characterize the surfaces of the contacting metals using scanning electron microscopy and scanning probe microscopy at various stages of the fabrication. Based on these results we developed methods to improve the morphology in order to realize more reliable metal-molecule contacts. It is shown that improvement of the surface topography of the metals indeed leads to metal-molecule-metal junctions with a very low failure rate. © *2005 American Vacuum Society.*
[DOI: 10.1116/1.2130353]

I. INTRODUCTION

Electrical contacts between soft and hard materials pose a huge challenge for today's nanoscale fabrication techniques. Such contacts are necessary prerequisites for molecular electronics as well as for the use of soft materials as active electrical elements on the Ångstrom scale. In recent years a large number of approaches have been attempted to find reproducible techniques for generating such contacts.[1–4] The patterning of small contacts to a thin molecular layer is difficult because most lithographic techniques are invasive to molecular materials. Electron beam lithography includes the deposition of a resist and the exposure of the substrate to high energy electrons. The transfer of patterns into the molecular layer by etching techniques is also not feasible because of the very small thickness of the molecular layers.

Conventional fabrication methods can be used to generate evaporated metal contacts to measure transport properties in polymer layers. However, application of these schemes to contacts to single or a few molecules is not straightforward. A large number of experiments have been reported using this approach.[5–9] The results, however, seem to vary broadly and uncontrollably. This variation is probably related to variations in exact contact geometry on the Ångstrom scale. Many approaches exploit properties of the fabrication of a self assembled monolayer (SAM) deposited on top of an evaporated electrode. The second electrode is either formed by evaporation on top of this electrode or by contacting single molecules using scanning probe microscopy (SPM). Reliable contacts to SAMs using SPM are difficult to realize.[10] Contacting pure SAMs suffers from strong interactions between the SPM-tip and the molecules and intermolecule interactions. Contacting single molecules, which are deposited in a matrix of nonconductive molecules, appears to be more reliable.[10] One method for obtaining stable current-voltage (*I-V*) curves is to deposit small gold clusters on top of the molecules and to achieve electrical contact through this cluster to the molecules. In all these cases a strong asymmetry exists in the contacts that complicates the interpretation of the *I-V* curves.

Evaporation of the second electrode on top of SAMs is a useful tool to characterize molecules on larger scales.[11] It is, however, sensitive to the formation of shorts through pinholes in the SAM. Therefore techniques have to be developed that either allow contacting the SAM on a very small length scale or depositing the top electrode in a way that does not cause formation of these shorts. In this article we demonstrate two different approaches for the counterelectrode deposition. In the first case a small area contact is created by evaporation through a shadow mask. The critical features of the mask are produced before depositing the monolayer. In the second case counterelectrode deposition is

a)Electronic mail: artur.erbe@uni-konstanz.de

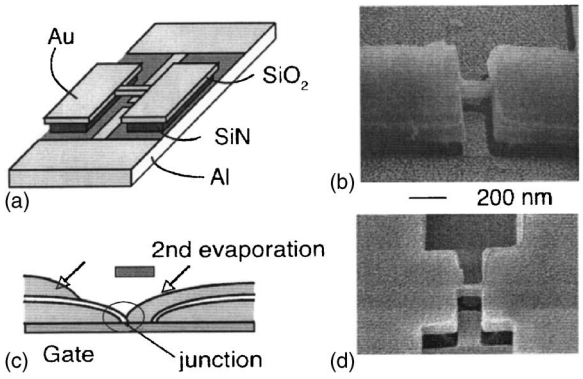

FIG. 1. Production of shadow mask on silicon substrate. (a) The shadow mask is defined via EBL in a $Si_3N_4-SiO_2$ double layer using two dry etching steps. (b) The bridge in the center of the structure is used to separate two metal contacts, which are evaporated vertically onto the substrate. A SAM is deposited on both electrodes. In a second step metal is evaporated under an angle that allows a small overlap between this top electrode and one of the bottom electrodes. If this overlap is small enough, transport through single or a few molecules can be possibly measured. (c) SEM picture of the mask on a silicon substrate after evaporation of the bottom electrodes. The dry etching creates a rough SiO_2 surface. This roughness causes the rough surface topography of the metal seen in the SEM picture. (d) A similar mask produced on a mica substrate. In this case the roughness of the electrodes is reduced.

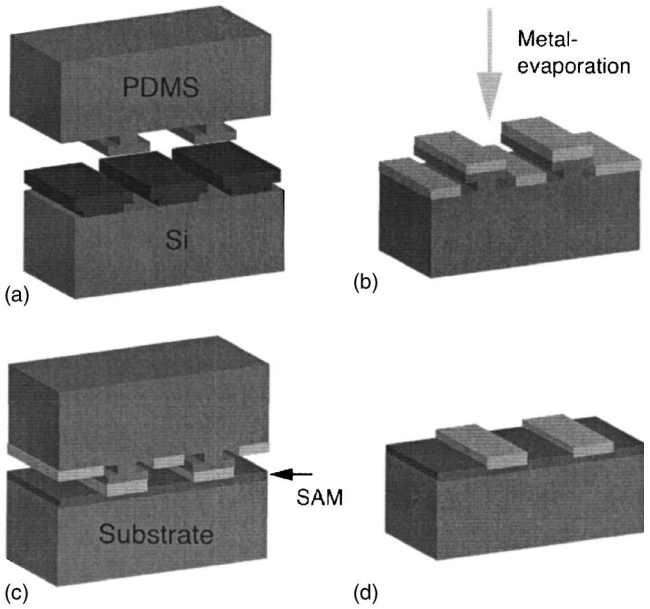

FIG. 2. Production of nanoscale features by nano transfer printing (nTP). (a) The features are defined by EBL in a PMMA double layer on a silicon substrate. The PDMS is cast into the structures and cured at 60 °C. Fluorination of the substrate before this step ensures easy separation of PDMS and substrate after the curing. (b) Layers of 10–30 nm metal (gold) are evaporated onto the PDMS stamp. (c) Alkane-di-thiols form a monolayer on a GaAs substrate. The gold on the PDMS stamp binds to this monolayer and is transferred to the substrate. (d) The patterned gold film that forms is transferred on top of the GaAs substrate. Good binding to the monolayer is proved by the scotch tape test.

performed using a structured poly(dimethylsiloxane) (PDMS) stamp. In this case all critical size features are defined on the stamp before it is brought into contact with the molecules. Both techniques thus allow us to protect the molecules from the invasive fabrication used for defining the critical size features.

II. SAMPLE PREPARATION

Fabrication of the shadow masks is sketched in Fig. 1. The masks are fabricated either on a silicon substrate or on freshly cleaved mica. The scheme allows for incorporation of a gate electrode underneath the junction. In order to reduce leakage from the gate to the metal contacts we use a narrow (5 μm wide) aluminum line, which is covered by SiO_2, as a gate electrode. Optical lithography is used to define the large metallic contacts, which are used to either attach wires or contact the junctions in a cryogenic probe station. The shadow mask materials, a double layer of Si_3N_4 and SiO_2, are deposited by plasma enhanced chemical vapor deposition (PECVD). We use electron beam lithography (EBL) to define two narrow lines (100 nm wide) separated by a 100 nm gap. This structure is etched anisotropically into the SiO_2 layer using reactive ion etching (RIE). The process gas for this step is CF_4. RIE with CHF_3 as a process gas etches Si_3N_4 isotropically and is therefore used to suspend the SiO_2 in the small gap between the two lines. Thus a bridge structure is fabricated as shown in Fig. 1(a). We evaporate metal (gold in the case of the pictures shown) perpendicular to the sample surface. This step creates two metal electrodes on the bottom SiO_2 separated by the width of the bridge (100 nm).

The sample is then soaked in a solution of di-thiol molecules for 30 min up to several hours. Molecules in our experiments are either terphenyldithiol or terthiophenedithiol. The molecular solution is a tetrahydrofuran (THF) solution of the molecules (about 0.01 mM). A few drops of 37% aqueous solution of ammonium hydroxide are added in order to deprotect the thiol endgroups. After the assembly of the molecular monolayer the sample is rinsed in THF, acetone, and Isopropanol. This procedure requires mask and substrate materials that are inert against all the solvents used during the assembly of the molecules.

In the final step we evaporate a second metal layer at an angle of $30°-40°$ onto the sample. This ensures a small overlap (about 50×50 nm^2) between the second metal layer and the left of the bottom electrodes [as shown in Fig. 1(b)]. The second electrode is shorted to the right electrode due to the large area of overlap. The metal layer deposited on top of the shadow mask is electrically disconnected because of a well defined undercut in the shadow mask. We can then characterize the electrical transport from the left electrode through the SAM to the right electrode. In order to study the influence of the topography of the contacting electrodes, the surface roughness of the contacting gold will be studied using scanning electron microscope (SEM) techniques. Studies on the topography of gold films evaporated on top of a SAM are presented elsewhere.[12]

The fabrication of nanoscaled patterns using nanotransferprinting (nTP)[13] is sketched in Fig. 2. In the first step we fabricate high resolution elastomeric PDMS stamps.[14] The prepolymer is either casted against a silicon wafer to produce

bulk flat gold or against a patterned master sample which was defined by EBL in order to define metal structures such as nanoscale lines or dots. In order to prevent sticking of the PDMS stamp to the wafer surface we first let a monolayer of (Tridecafluoro-1,1,2,2-Tetrahydrooctyl)trichlorosilane evaporate onto the wafer. Curing of the prepolymer takes place at 60 °C. For the definition of small patterns we use a double-layer poly(methyl methacrylate) (PMMA) (50 nm thick film bottom layer made from a 50 K PMMA in anisole and a 50 nm thick film top layer made with a 950 K PMMA in xylene). The bilayer *e*-beam resist produces an undercut profile in the patterns. This was done to form T tops in molded PDMS structures. A thin layer (about 3 μm thick) of hard PDMS[15] is then spun onto the sample and precured. The mechanical stability of the hard PDMS is larger than of the generic PDMS. It can therefore be used to define features with feature sizes down to 50 nm and aspect ratios of about 1:1. Casting of the soft PDMS on top of this layer and subsequent curing combines the soft and the hard PDMS layer. We then remove the PDMS from the wafer and evaporate metal on top of the PDMS surface that was formed by contact with the wafer. This metal is either characterized by SEM directly on the stamp or transferred to a suitable substrate and characterized by SEM and SPM.

III. CHARACTERIZATION OF GOLD LAYERS

A quantitative analysis of the morphology of the gold layers is difficult to achieve. SPM techniques are limited to the top surfaces of hard materials, and therefore not suitable for studies of the metal morphology on PDMS. We therefore concentrate mainly on features that can be seen in SEM pictures of the metal surfaces at various stages of the production process. Gold layers in the shadow mask structure are characterized before the assembly of the molecular monolayer. Typical examples of such gold layers can be seen in Figs. 1(c) and 1(d). The SiO_2 layer under the shadow mask is affected by the final dry etching process. This leads to an increased roughness of the bottom electrode if the structure is produced on a silicon substrate [shown in Fig. 1(c)]. A large number of junctions showed conductivity values below 0.5 nS. Furthermore current levels in the junctions with conductivities above 1 nS are lower than in previous reports of junctions prepared in a different geometry using identical molecules.[2,16,17] The qualitative behavior of the junctions is similar, however. This can be explained if we assume that similar states in the molecular monolayer are contacted with the two different techniques. The quality of the coupling, however, is changed in the shadow mask technique due to the surface roughness of the bottom gold.

The roughness of the bottom electrode can be reduced by fabricating junctions on substrates that are not affected by the final dry-etching step. Examples are mica and silicon coated with a thin layer of SU-8. Figure 1(d) shows that in this configuration the bottom electrode looks much smoother than on bare silicon. Residual stress between the mask and the underlying material, however, created structural failures and short circuits between the metal layer on top of the mask

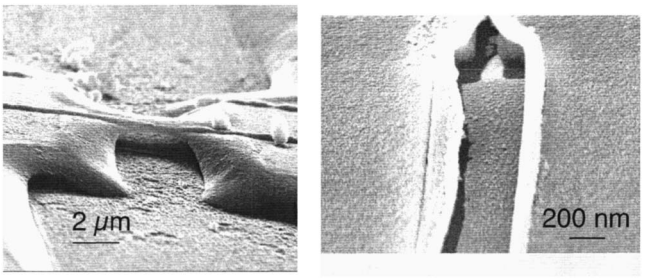

FIG. 3. Effects of stress on the shadow masks. (a) Metallic (Ni) shadow mask on a silicon substrate. The mask is separated from the substrate by a hard baked resist layer. This combination of materials leads to large stress. The undercut metal edges of the mask fall down. (b) Small imperfections in the $Si_3N_4-SiO_2$ layer can lead to failure in the edges of the mask shown in Fig. 1. Both failures shown in (a) and (b) lead to short circuits between the bottom electrode and the metal layer on top of the masks.

and the electrodes on the substrate for all measured samples [a typical example is shown in Fig. 3(a)]. Figure 3(b) shows that broken edges of the mask can also be caused by small imperfections of the pure $SiO_2-Si_3N_4$ mask. Therefore a reliable fabrication scheme is necessary for optimal yield of good junctions.

The roughness of the bottom gold can be also decreased by thermal annealing of the gold. Figure 4 shows the effect of this step. In Fig. 4(a) a junction which was not annealed but otherwise produced in an identical way is shown. The grains of the bottom gold can be clearly resolved in the SEM micrograph. All junctions that were produced without annealing in this geometry (which is a slightly altered version of the geometry shown in Fig. 1) were shorted between the top and the bottom metal. After the annealing step [Fig. 4(b)] the height of the grains in the bottom layer was reduced. Therefore the contrast of the grains is lowered in the SEM picture. SPM studies of similar samples confirm this observation. In this case a much larger number of unshorted samples was found (almost 100% of the samples, if gold was used as a top metal electrode). Histograms of the conductivity values for samples fabricated with and without the annealing step are shown in Fig. 4. The annealed sample shows a low number of junctions with resistance below 10^3 Ω (contact leads resistance).

The importance of the topography of the metal surfaces in the shadow-mask geometry motivated studies of the metal morphology in the nTP process at various stages. The experiments concentrate on the morphology of the gold on the PDMS stamps and after printing on the substrate. We use a variety of processing steps in order to investigate the influence of residual stress on this morphology.

For unpatterned gold samples we investigate the morphology of the gold on the PDMS as well as the printed gold on alkane-di-thiol SAMs on GaAs. SPM studies of printed nanostructured gold on GaAs was done and is published in a separate publication.[12] For nanostructured gold contacts defined by nTP it is important that the structures are electrically

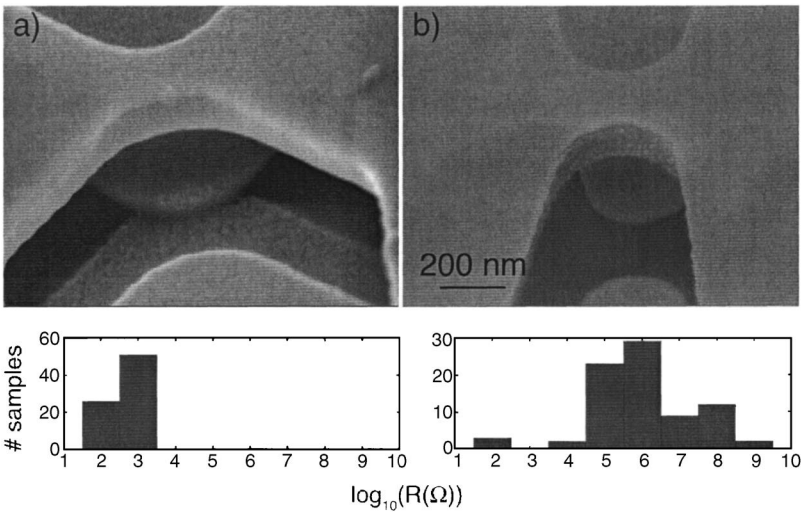

FIG. 4. Effects of annealing on the bottom gold layer. (a) Junction built on the gold layer as deposited. The roughness of the gold can be clearly seen. 100% of junctions prepared without annealing are shorted in this geometry regardless of the molecules or top metals used. (b) Bottom electrode annealed at 300 °C. It can be seen that the surface of the gold shows larger and flatter grains than before the annealing. This leads to a dramatically decreased number of shorts between the two electrodes, which is illustrated in the two histograms shown below the SEM pictures.

continuous. In the following we therefore concentrate on the control of cracks in the metal layer that can cause the structures to be disconnected.

Figure 5 shows the morphology of gold structures after the deposition of gold using various treatments of the PDMS. SEM pictures in Figs. 5(a) and 5(b) depict gold on a PDMS stamp, which has been treated by an argon plasma (gas flow approximately 30 sccm at a power of 100 W for 10–40 s) for 20 and 40 s, respectively. The argon bombardment causes some of the bonds in the surface of the PDMS to break. This can allow the material to relax the stress on the surface before crosslinking takes place again.[18] Both images are taken in an area where no residual stress in the PDMS is present, i.e., the pictures are taken far away from the clamp holding the PDMS stamp in the SEM. The main differences are the number and the size of the cracks in the gold on the PDMS obtained in the two cases. In the case of 20 s treatment, the cracks have distances ranging from 50 to 150 nm, while the cracks in the case of 40 s treatment have smaller distances, ranging down to about 25 mm in diameter, but are also less pronounced.

If the stamp is treated with an oxygen plasma prior to the deposition of the gold the number of cracks decreases drastically [Fig. 5(d)]. On the other hand, the width of the cracks increases. Transfer of these gold layers to the substrates, however, is impossible. It has to be noted that gold layers can be easily transferred from PDMS stamps, which have been treated with oxygen plasma for short times only (approximately 3–5 s). It is possible that the adhesion of gold atoms improves due to the oxygen plasma. This can lead to a decreased number of cracks because the gold layer cannot conform with the stress coming from the mismatch between PDMS and bulk gold on a small scale. This would also explain the poor transfer of these gold layers to the SAM. The interaction between the gold and the PDMS can be too strong for the gold-thiol endgroup interaction to overcome.

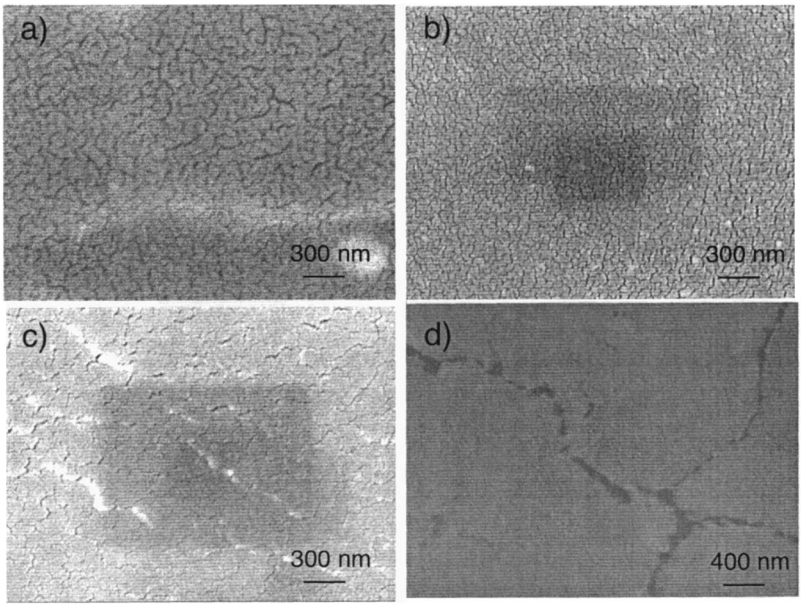

FIG. 5. Characterization of gold evaporated on PDMS under various conditions: (a) 10 nm of gold on a PDMS stamp, which was treated by an argon plasma for 20 s, (b) 10 nm of gold on a PDMS stamp, which was treated by an argon plasma for 40 s, (c) 10 nm of gold evaporated in three layers (of about 3 nm each), which are separated by alkane-thiol monolayers, and (d) 10 nm of gold after treatment of the PDMS stamp by an oxygen plasma for 10 s. Transfer of this gold layer to a substrate was impossible.

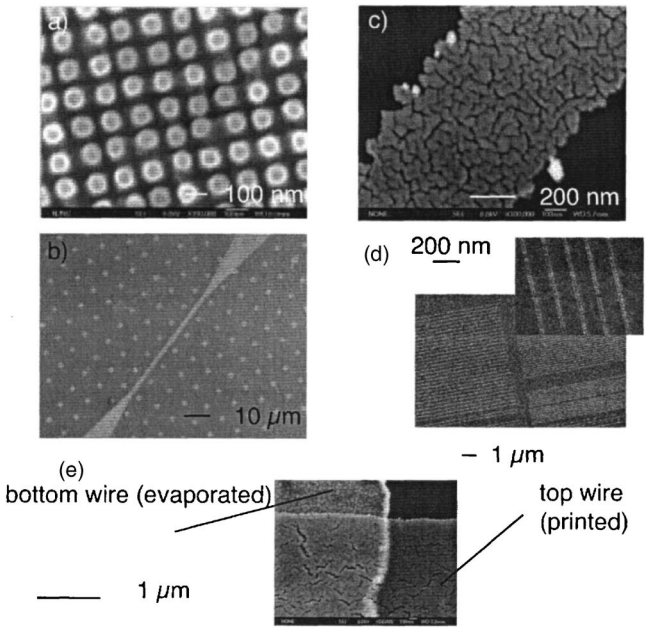

FIG. 6. Patterns generated by nTP: (a) gold dots of 100 nm diameter, (b) continuous gold line, (c) microscopic cracks seen at larger magnification do not break the electrical continuity of the wide lines, (d) narrow lines, which are disconnected due to cracks in the metal layer, and (e) cross junction of bottom evaporated gold line with a top printed electrode. The SAM on top of the bottom electrode serves both as electrical isolation and binding partner for the top electrode.

In order to transfer patterns of good quality to the molecular layers, the metal layer should have a low number of cracks and only a small influence of the gold grains. In order to achieve this the stress inside the metal layer coming from the contacts on both sides (to the PDMS or to the SAM) needs to be relaxed. In our experiments we evaporate thin ($\approx$3 nm) metal layers interchanging with SAMs of alkanethiols. The SAMs are evaporated onto the metal layers from a concentrated molecular solution inside a desiccator (evaporation times longer than 10 h). After this evaporation we rinse the metal layers on top of the stamps carefully with ethanol, in order to ensure coverage of a monolayer only. The stamps are immediately transferred into the evaporator and the next metal layer is evaporated. To release the stress in the metal layers the evaporation of molecular monolayers and thin metal layers is repeated until the desired metal thickness is reached. The samples shown in this article have a total metal thickness of 10 nm (consisting of three layers of 3.3 nm each). The SAM does not lead to an electrical isolation of the metal layers because the number of shorts is large due to the large area of overlap. Additional monolayers of molecules between the metal layers clearly decrease the size and the number of cracks in the gold on top of the PDMS, as can be seen in Fig. 5(c). We interpret this effect as a result of the stress relief in the soft monolayer that allows the gold atoms to rearrange. Printing of these layers is still possible to alkane-di-thiol monolayers on top of GaAs substrates.

The ultimate test for the quality of the metal layer is the transfer to the substrate using patterned PDMS stamps (nTP). In Fig. 6 we show a variety of printed patterns. Printed nanodots allow contacting molecules on a small area by SPM techniques. Conducting AFM or STM can both be used to investigate the *I-V* characteristics of the metal–SAM–metal junction formed by this configuration. Further experiments will be done comparing single-grain and multigrain dots to investigate the influence of grain boundaries.

In Fig. 6(d) a number of printed narrow (100 nm wide) lines are shown. The magnification shown in the inset illustrates the destructive effects of cracks in the metal layer on these narrow lines. We show in Fig. 6(e) that it is possible to create junctions by printing a wire on top of a thermally evaporated bottom wire. In order to produce this structure we define the bottom wire on a GaAs substrate by conventional EBL followed by a metal liftoff. A SAM is subsequently assembled on top of the wire as well as on the bare GaAs by soaking the substrate in a alkane-di-thiol solution overnight. The stamp is produced with three metal layers and two SAMs, as described above. We use a microscope to align the stamp with the structured substrate and transfer the metal on the stamp to the substrate. The resulting structure is shown in Fig. 6(d). Electrically this structure shows a short between the upper layer and the lower gold layer. This demonstrates that we can indeed combine photolithography and nTP to produce a top layer that is continuous even over the edges of the lower metal stripe. However, in order to measure conductivity through a molecular layer the area of overlap has to be reduced further in order to reduce the number of contacted pinholes in the bottom layer and the topography of both layers has to be optimized.

IV. CONCLUSION

We have presented two ways to structure nanoscale junctions for molecular electronics using shadow evaporation and nanocontact printing. It has become obvious that every contacting technique depends on the quality of the involved metal layers. This implies that studies of the morphology of the metals at various stages of the fabrication are absolutely necessary in order to understand possible issues that can lead to unreliable structures. The main challenge is imposed by the need to have the hard metal make intimate contact with the rather soft and thin molecular layers. Both materials form structures on their typical length scales. Thus the fabrication method has to give the materials the opportunity to relax at the interface. In the case of the shadow mask fabrication of small junctions, the grain formation of the bottom electrode strongly effects the *I-V* characteristics of the junctions. Using thermal annealing of the contacting electrodes, an extremely reliable contacting method was found. For the fabrication of nanoscale patterns using nTP, a softening of the metal on the PDMS stamp seems to improve the quality of the printed metal. In future experiments we will characterize these printed junctions electrically. The use of these different contacting techniques on the same molecular layers will reveal properties of the metal-molecule contacts. Further steps will then lead to the design of a reliable contact, which is necessary to probe the electrical properties of the molecules.

[1]H. Park, A. Lim, A. Alivisatos, J. Park, and P. McEuen, Appl. Phys. Lett. **75**, 301 (1999).
[2]N. Zhitenev, H. Meng, and Z. Bao, Phys. Rev. Lett. **88**, 226801 (2002).
[3]J. Chen, M. Reed, A. Rawlett, and J. Tour, Science **286**, 1550 (1999).
[4]M. Reed, C. Zhou, C. Muller, T. Burgin, and J. Tour, Science **278**, 252 (1997).
[5]J. Park *et al.*, Nature (London) **417**, 763 (2002).
[6]H. Park, J. Park, A. Lim, E. Anderson, A. Alivisatos, and P. McEuen, Nature (London) **407**, 57 (2001).
[7]W. Liang, M. Shores, M. Bockrath, J. Long, and H. Park, Nature (London) **417**, 725 (2002).
[8]J. Reichert, R. Ochs, D. Beckmann, H. Weber, M. Mayor, and H. v. Löhneysen, Phys. Rev. Lett. **88**, 176804 (2002).
[9]S. Kubatkin, A. Danilov, M. Hjort, J. Cornil, J.-L. Brèdas, N. Stuhr-Hansen, and P. Hedeg, Nature (London) **425**, 698 (2003).
[10]X. Cui, A. Primak, X. Zarate, J. Tomfohr, O. Sankey, A. Moore, T. Moore, D. Gust, G. Harris, and S. Lindsay, Science **294**, 571 (2001).
[11]B. de Boer, H. Meng, D. Perepichka, J. Zheng, M. Frank, Y. Chabal, and Z. Bao, Langmuir **19**, 4272 (2003).
[12]W. Jiang, N. Zhitenev, Z. Bao, H. Meng, D. Abusch-Magder, D. Tennant, and E. Garfunkel, Langmuir **21**, 8751 (2005).
[13]Y. Loo, R. Willett, K. Baldwin, and J. Rogers, Appl. Phys. Lett. **81**, 562 (2002).
[14]Sylgard 184, Dow Chemical Co.
[15]T. Odom, J. Love, D. Wolfe, K. Paul, and G. Whitesides, Langmuir **18**, 5314 (2002).
[16]N. Zhitenev, A. Erbe, H. Meng, and Z. Bao, Nanotechnology **14**, 254 (2003).
[17]N. Zhitenev, A. Erbe, and Z. Bao, Phys. Rev. Lett. **92**, 186805 (2004).
[18]F. Katzenberg, Nanotechnology **14**, 1019 (2003).